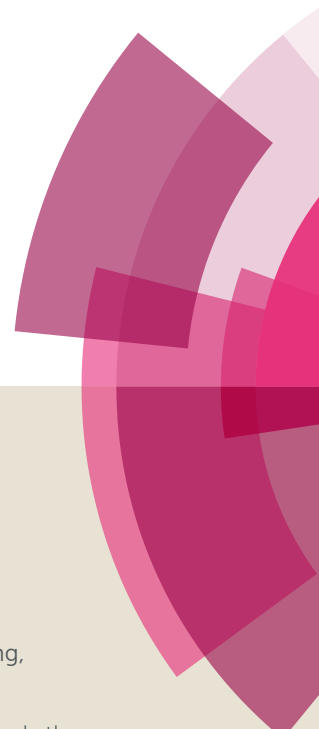


NJC

Accepted Manuscript



This article can be cited before page numbers have been issued, to do this please use: B. Tang, W. Song, S. Li, E. Yang and X. Zhao, *New J. Chem.*, 2018, DOI: 10.1039/C8NJ02449A.



This is an Accepted Manuscript, which has been through the Royal Society of Chemistry peer review process and has been accepted for publication.

Accepted Manuscripts are published online shortly after acceptance, before technical editing, formatting and proof reading. Using this free service, authors can make their results available to the community, in citable form, before we publish the edited article. We will replace this Accepted Manuscript with the edited and formatted Advance Article as soon as it is available.

You can find more information about Accepted Manuscripts in the [author guidelines](#).

Please note that technical editing may introduce minor changes to the text and/or graphics, which may alter content. The journal's standard [Terms & Conditions](#) and the ethical guidelines, outlined in our [author and reviewer resource centre](#), still apply. In no event shall the Royal Society of Chemistry be held responsible for any errors or omissions in this Accepted Manuscript or any consequences arising from the use of any information it contains.

Post-synthesis of Zr-MOR as robust solid acid catalyst for the ring-opening aminolysis of epoxides

Bo Tang,^a Wei-Chao Song,^a Sheng-Yang Li,^a En-Cui Yang*^a and Xiao-Jun Zhao*^{a,b}

^aKey Laboratory of Inorganic-Organic Hybrid Functional Material Chemistry, Ministry of Education, Tianjin Key Laboratory of Structure and Performance for Functional Molecules, Tianjin Normal University, Tianjin 300387, People's Republic of China

^bDepartment of Chemistry, Collaborative Innovation Center of Chemical Science and Engineering, Nankai University, Tianjin 300071, People's Republic of China

*Corresponding author

E-mail address: encui_yang@163.com and xiaojun_zhao15@163.com

Abstract: Zirconosilicate with the MOR topology (Zr-MOR) was successfully prepared using a two-step post-synthesis strategy from pre-dealumination of H-MOR zeolite and subsequent dry impregnation of Cp_2ZrCl_2 . Incorporated Zr species mainly existed in the form of isolated tetrahedrally coordinated Zr in MOR framework. It was found that the mechanism of post-synthetic incorporation of Zr involved interaction between the Cp_2ZrCl_2 molecules and silanols at defects generated by steaming and acid treatment. In comparison with Ti- and Sn-silicate analogues, as-synthesized Zr-MOR zeolite showed high activity and regio-selectivity in the ring-opening aminolysis of epoxides to the β -amino alcohols under ambient and solvent-free conditions, which was related to the impact of Lewis acid sites of catalysts, the basicity of amines and competitive adsorption of reactant molecules. Moreover, Zr-MOR zeolite could be reused at least five cycles without loss of activity and

regio-selectivity.

Keywords: Zirconosilicate; Ring-opening aminolysis; Epoxides; Post-synthesis; β -amino alcohols

1 Introduction

Epoxides are significant important synthetic intermediates, which can be industrially obtained from the corresponding olefin precursors [1,2]. Due to their three-membered heterocyclic ring strain, epoxides are susceptible to attacks by a range of nucleophiles, such as amines, alcohols, azides and thiols, leading to bifunctional molecules for great chemical industry. For instance, β -amino alcohols, obtained by the ring-opening of epoxides with amines, are used as versatile intermediates for the synthesis of various biologically active natural products, unnatural amino acids, β -blockers, insecticidal agents, chiral auxiliaries, oxazolines, *etc.* [3-6]. To date, several homogeneous catalytic system including metal triflates, metal halides, sulfamic acid and ionic liquids have been applied to realize the ring-opening of epoxides [7-11]. However, most of the homogeneous catalytic process suffer from several disadvantages, *e.g.* the use of halogenated and/or toxic solvents, the difficulty of separation, poor regio-selectivity and reusability issue. Therefore, for potential applications in industry, it is highly desirable and necessary to develop robust solid catalysts with environmental friendliness, high activity and regio-selectivity as well as good recyclability for this transformation [12-16].

Zeolites have been widely utilized for diverse applications, such as catalysis, separation, ionic exchange, *etc.* because of their crystalline structures, uniform pore channels and high surface area [17-21]. Incorporation of metal ions, *e.g.* Ti^{4+} , Sn^{4+} and Zr^{4+} , into zeolites framework endows traditional zeolites with many interesting properties, making them ideal heterogeneous catalysts for a great many of green chemical transformations [22-24]. Recently, mesoporous titanosilicates and microporous TS-1, as solid Lewis acids, have been found to be active in the

ring-opening aminolysis of epoxides reaction [25-27]. Attempts are also made to synthesis nanocrystalline zirconosilicates and applied as promising candidates for the ring-opening of epoxides with amines and alcohols [28]. In spite of the attractive catalytic performance achieved, the types of metallosilicates for the ring-opening of epoxides reaction were still scarce, and mainly focused on MFI framework structure [25,28]. Hence, researches on ring-opening of epoxides involving metallosilicates as catalysts are only in its infancy, and new types of metallosilicates are urgently required to be further developed.

MOR-type zeolite can be facilely synthesized *via* hydrothermal method even without any organic structure-directing agent, and serves as effective solid acid catalyst in petrochemical industry [29]. However, there is, up to now, no literature reporting the successful direct synthesis of metallosilicates based on MOR framework. This is because the synthesis system for MOR-type aluminosilicate (alkaline metals and high Al content) make it difficult to incorporate heteroatom into the MOR zeolite directly. Post-synthesis strategies have been recently proposed as an alternative choice for the development of metallosilicates with high catalytic efficiency [30-35]. Our previous work reported an improved two-step post-synthesis strategy for the preparation of Sn-Beta zeolite, which was more active than the hydrothermally synthesized one in the Bayer-Villiger oxidation and dihydroxyacetone conversion into methyl lactate reaction [36]. In this context, we, herein, will report a two-step post-synthesis procedure for the preparation of Zr-MOR zeolite, involving dry impregnation of dealuminated MOR zeolite with organometallic precursor Cp_2ZrCl_2 . The properties of the Zr-MOR zeolite were characterized and the catalytic performance was investigated in detail for the ring-opening of epoxides with amines reaction.

2 Experimental

2.1 Sample preparation

Zr-MOR zeolite was synthesized *via* a simple and scalable post-synthetic strategy previously employed for Sn-Beta [36], Ti-Beta [37] and Zr-Beta [38], that is,

dealumination of parent H-MOR zeolite and dry impregnation of Zr species into the zeolite framework. Briefly, commercial H-MOR with a $n_{\text{Si}}/n_{\text{Al}}$ ratio of 11 (Nankai University Catalyst Co., Ltd.) was firstly calcined in air at 973 K for 10 h, then followed by acid reflux with 13 mol L⁻¹ nitric acid aqueous solution (20 mL g⁻¹ zeolite) at 373 K for another 10 h. The mixture was filtrated, thoroughly washed with deionized water, and dried at 373 K overnight. For dry impregnation of Zr, dealuminated MOR was pre-treated at 473 K overnight under vacuum to remove physisorbed water. Then, 1.0 g of resultant powder and certain amount of Cp₂ZrCl₂ (*i.e.* 0.024, 0.048, 0.096 and 0.192 g) were ground in agate mortar for 10 min, followed by transfer into a tubular reactor and calcined at 823 K for 6 h (heating rate at 5 K min⁻¹) under flowing air to obtain the final Zr-MOR-*X* zeolites where *X* stands for the $n_{\text{Si}}/n_{\text{Zr}}$ ratio of 200, 100, 50 and 25, respectively. It should be noted that Zr-MOR in this study generally refers to Zr-MOR-100 unless otherwise specified.

2.2 Characterization techniques

Powder X-ray diffraction (XRD) was recorded on a Bruker D8 diffractometer with Cu-K α radiation ($\lambda = 1.54184 \text{ \AA}$) from 5° to 40° with a scan speed of $2\theta = 6.0^\circ \text{ min}^{-1}$. SEM images of the samples were acquired on a Nova Nano 230 scanning electron microscope. Surface areas and pore volumes were measured by means of nitrogen adsorption at 77 K on a Micromeritics ASAP 2020 after activating the samples at 473 K for 6 h. The total surface area was calculated *via* the Brunauer–Emmett–Teller (BET) equation, and the microporous pore volume was determined using the *t*-plot method. The chemical compositions were detected by inductively coupled plasma atomic emission spectrometry (ICP-AES) on a Thermo IRIS Intrepid II XSP atomic emission spectrometer. Fourier transform infrared (FT-IR) spectroscopy was recorded on a Bruker Tensor 27 spectrometer with 32 scans for a resolution of 4 cm⁻¹ in KBr medium at room temperature. Diffuse reflectance infrared Fourier transform (DRIFT) spectra were performed on a Bruker Tensor 27 spectrometer with 128 scans at a resolution of 2 cm⁻¹. A self-supporting pellet made of sample material was placed in the reaction chamber and calcined in flowing dry Ar at 673 K for 2 h before collecting the spectra. Diffuse reflectance ultraviolet-visible (UV-vis) spectra were recorded

against BaSO₄ on a Hitachi U-4100 UV-vis spectrophotometer. X-ray photoelectron spectra (XPS) were recorded on a Kratos Axis Ultra DLD spectrometer with a monochromated Al-K α X-ray source ($h\nu = 1486.6$ eV), hybrid (magnetic/electrostatic) optics and a multi-channel plate and delay line detector (DLD). All spectra were recorded using an aperture slot of 300 \times 700 microns. Survey spectra were obtained with a pass energy of 160 eV and high-resolution spectra were obtained with a pass energy of 40 eV. Accurate binding energies (± 0.1 eV) were determined based on the position of the adventitious C 1s peak at 284.6 eV. CasaXPS software was used for spectra analysis.

2.3 Catalytic evaluation

Catalytic ring-opening aminolysis of epoxides was carried out in a 10 mL round-bottom glass flask. The vessel was charged with a mixture of equimolar quantities of epoxide and amine (5 mmol) and 25 mg of catalyst, and mixed vigorously using a magnetic stirrer. After each reaction, aliquots of the reaction medium were taken out and diluted with a known quantity of dichloromethane, then subjected to a Agilent GC 7890B (Agilent HP-5 column, 30 m \times 0.25 mm \times 0.25 μ m; FID detector) to monitor the reaction process. The GC peaks were identified by comparison with the retention times of the known standard samples, and by means of a Shimadzu GC-MS QP2010 SE equipped with an Agilent HP-5MS column.

3 Results and discussion

3.1 Incorporation of Zr into zeolite framework

The XRD patterns of parent H-MOR and the corresponding post-treated deAl-MOR and Zr-MOR samples were shown in **Fig. 1a**. It was obvious that similar diffractions attributed to a typical MOR topology with the comparable intensity could be observed for the three samples, indicating no destruction of zeolite framework during the dealumination and Zr incorporation procedures, in accord with previous literatures [39,40]. The steaming and acid treatment led to an obvious shift of the diffraction peak (200) to higher angle (**Fig. 1b**), revealing the contraction of the MOR matrix upon relatively larger Al ions removal (in comparison to Si ions). Conversely,

the subsequent Zr incorporation process resulted in a shift of (200) peak to lower angle compared with the dealuminated sample. This was a clear evidence of MOR framework expansion due to much larger ionic radius of Zr ions, thus indicating the successful incorporation of Zr species into the framework of MOR zeolite. There was no characteristic reflections of crystalline zirconia (JCPDS# 04-001-7279) in the patterns of as-prepared Zr-MOR, suggesting that Zr was homogeneously dispersed during the dry impregnation procedure. The well-preserved microporous MOR structure after dealumination and Zr incorporation was further confirmed by possessing the same type I isotherms for parent H-MOR and the post-treated samples (Fig. S1).

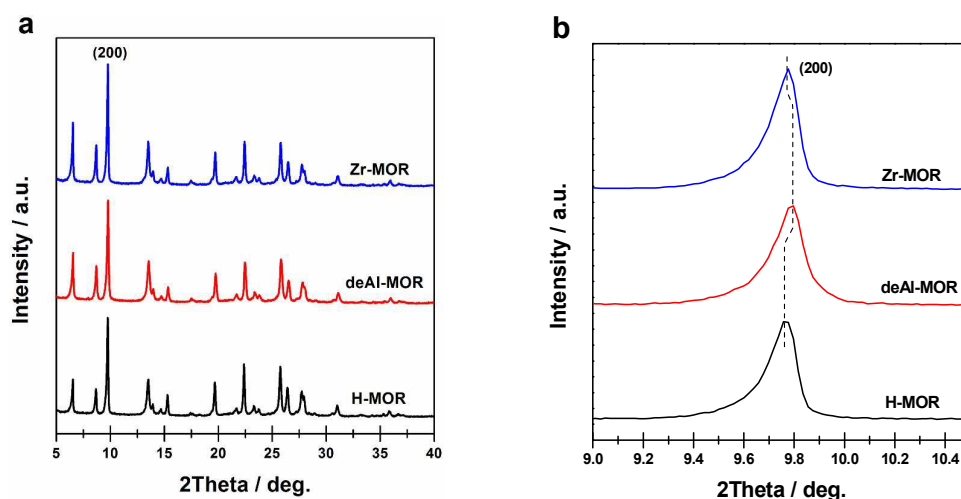


Fig. 1 Wide angle XRD patterns (a) and enlarged (200) reflections (b) of H-MOR, deAl-MOR and Zr-MOR.

SEM investigation was made to confirm the morphology of post-treated samples in this study. As shown in Fig. 2, parent H-MOR showed aggregates of small pseudo-rod shaped crystallites, and the same morphology were observed for the deAl-MOR and as-prepared Zr-MOR, demonstrating the preservation of zeolite framework after the dealumination and Zr incorporation processes. Atomic contents in Zr-MOR sample was obtained using EDX spectroscopy (Fig. S2), which confirmed the presence of Si, O, Al and Zr atoms. For a detailed distribution of atomic contents inside the nanocrystals, elemental mapping of Si and Zr was performed. The elemental mapping showed fairly homogeneous dispersion of Zr species in the case of Zr-MOR; no

particles of bulk zirconia were detected, in line with the XRD characterization.

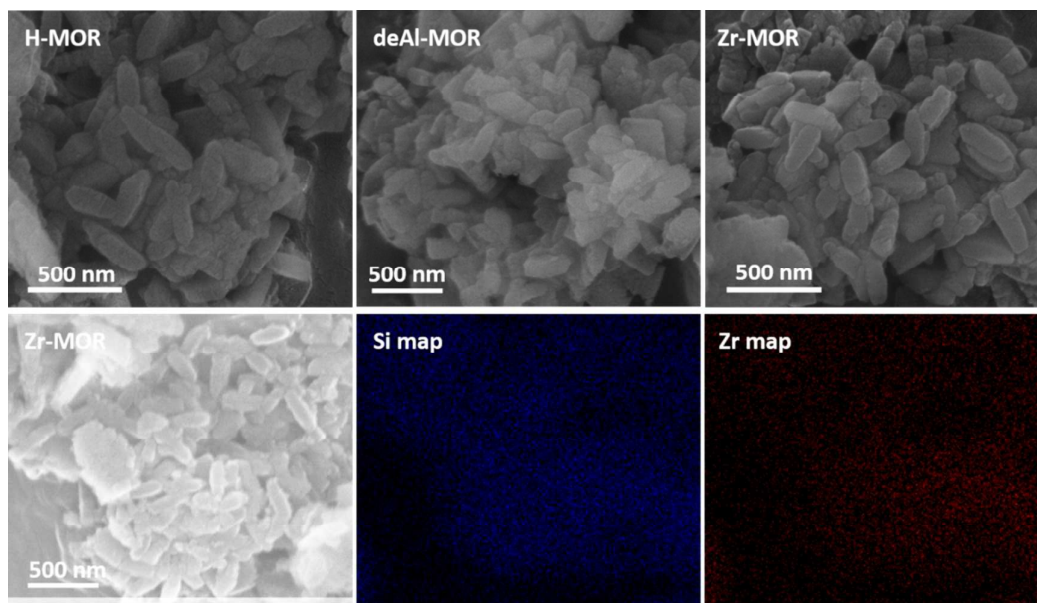


Fig. 2 SEM images and EDS mapping of Si and Zr for Zr-MOR.

The textural properties of H-MOR, deAl-MOR and Zr-MOR were listed in **Table 1**. The steaming and nitric acid treatment led to a distinct decrease in the n_{Si}/n_{Al} ratio from 11 for H-MOR to 160 for deAl-MOR, as a result of substantial Al from MOR framework. Interestingly, there was no obvious change in BET surface areas (370–397 $m^2 g^{-1}$) and microporous volumes (0.148–0.153 $cm^3 g^{-1}$), demonstrating that the dealumination and Zr incorporation procedures did not strongly affect the textural properties of MOR framework. The actual n_{Si}/n_{Zr} ratio of as-synthesized Zr-MOR was determined to be 97.0, in good agreement with the theoretical value of 100.

Table 1 Physicochemical properties of H-MOR, deAl-MOR, and Zr-MOR samples

Sample	n_{Si}/n_{Al} ^a	n_{Si}/n_{Zr} ^a	Surface area ^b ($m^2 g^{-1}$)	Pore volume ^c ($cm^3 g^{-1}$)
H-MOR	11	—	370	0.148
deAl-MOR	160	—	397	0.153
Zr-MOR	158	97.0	383	0.148

^a Determined by ICP. ^b Specific surface area obtained by the BET method. ^c Calculated from *t*-plot.

3.2 Existence states of Zr species in Zr-MOR

Diffuse reflectance UV-vis spectroscopy was widely utilized to disclose the site isolation and the coordination states of the transition metal species in zeolite. The UV-vis spectrum of Zr-MOR in **Fig. 3** showed a strong adsorption band at ca. 205 nm. This band can be ascribed to ligand-to-metal charge transitions from O^{2-} to dispersed Zr^{4+} ions, specially as the catalytically active isolated tetrahedrally coordinated Zr(IV) in zeolite framework [41-43]. Moreover, no bands related to bulk ZrO_2 reference could be examined in the Zr-MOR spectrum, suggesting the exclusion of aggregated ZrO_2 crystalline, which was in consistent with the characterization result from XRD.

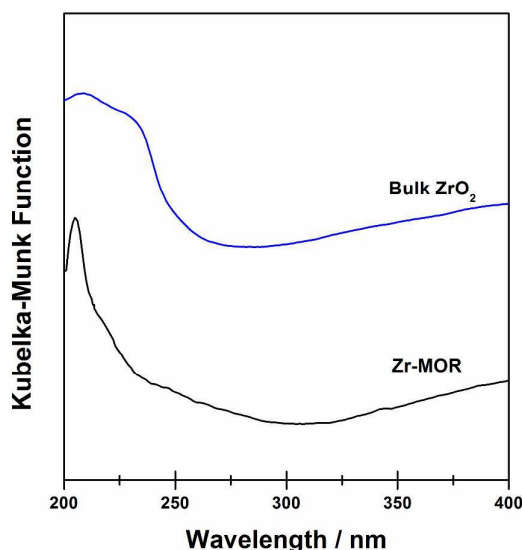


Fig. 3 UV-vis spectra of Zr-MOR and ZrO_2 .

For further insights into the local environment of the incorporated Zr species, XPS measurements were applied. As shown in **Fig. 4**, two signals referent to the Zr $3d_{3/2}$ and Zr $3d_{5/2}$ photoelectrons located at 185.1 and 182.7 eV, respectively, were emerged for Zr-MOR, much higher than that of the bulk ZrO_2 reference (184.6 and 182.2 eV). According to the previously reported work [44], the binding energy was shifted obviously to higher values could be seen as an indicator of the formation of Si–O–Zr bonds in the zeolite structure together with transformation of geometry from octahedral to tetrahedral-coordination. This result suggested that the incorporated Zr species in MOR framework mainly existed in the form of tetrahedrally coordinated state, in accordance with the UV-vis analysis. Similar results has also been reported for BEA- and MFI-type metallocates due to heteroatom incorporation into their

frameworks [44-46].

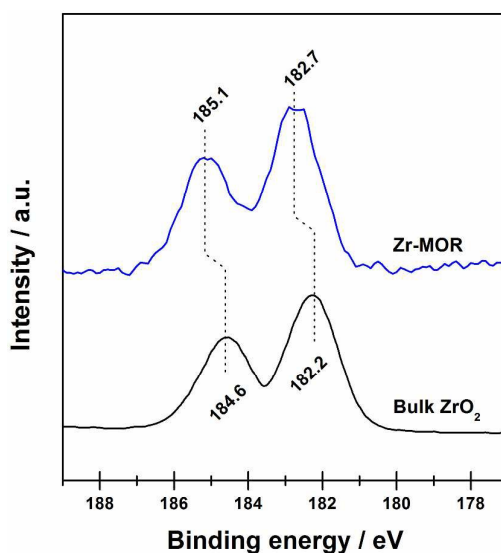


Fig. 4 Zr 3d XPS of Zr-MOR and ZrO₂.

3.3 The mechanism of Zr incorporation

On the basis of the characterization results discussed above, we assumed that the mechanism of post-synthetic incorporation of Zr atom into the framework of MOR zeolite involved creating defect sites associated with silanol groups through dealumination and subsequent interaction of these silanol groups with the corresponding metal precursor, thus resulting in tetrahedral metal sites incorporated into the zeolite framework, as graphically described in **Scheme 1**. Here, such a hypothesis was investigated based on infrared spectroscopy.



Scheme 1 Schematic representation of the incorporation of tetrahedral Zr(IV) into MOR framework.

Fig. 5a showed the FT-IR spectra of the parent H-MOR, deAl-MOR and Zr-MOR in the skeletal vibration region of 700–1400 cm⁻¹. A newly formed band located at 955

cm^{-1} was observed for deAl-MOR sample. According to the early study, it was associated with asymmetric vibration of the Si-OH bonds at defect sites [40]. An analogous phenomenon was also been observed for BEA zeolite due to the extraction of framework Al ions [36,37]. A distinct decline in the band intensity occurred as for the following dry impregnation with Cp_2ZrCl_2 . Simultaneously, a minor vibration band at 965 cm^{-1} appeared, which belonged to an asymmetric stretching mode of $[\text{O}_3\text{Si}-\text{O}-\text{Zr}]$ unit [28,48,49]. These results probably gave the support for the binding Zr at the defect sites and thus incorporation of Zr into the zeolite MOR framework.

To further investigate into this issue, the DRITF spectra in the hydroxyl stretching region of $3400\text{--}4000 \text{ cm}^{-1}$ of parent H-MOR, deAl-MOR and Zr-MOR were also performed and presented in **Fig. 5b**. In the H-MOR spectrum, three major bands at 3735 , 3650 and 3605 cm^{-1} , corresponding to external silanol groups, non-framework Al and bridging hydroxyls (Si-OH-Al), respectively, could be distinguished [39,50]. The treatment of H-MOR with steaming and concentrated nitric acid resulted in a great decrease in the intensity of framework Al-related 3650 and 3610 cm^{-1} bands. This indicated that a significant amount of Al ions were eliminated from the MOR framework, as confirmed by the ICP analysis (**Table 1**). Meanwhile, the appearance of two new bands at 3725 and 3578 cm^{-1} derived from the internal silanol groups were observed after the dealumination process [36,51,52], confirming the formation of defect sites in the zeolite framework. Specifically, the broad feature of the 3578 cm^{-1} band indicated that it was attributed to hydrogen-bonded silanols, which located at the defect sites of dealuminated MOR framework in the form of hydroxyl nests. After dry impregnation of Cp_2ZrCl_2 , the bands at 3725 and 3578 cm^{-1} associated with internal silanols decreased in intensity, hinting that Cp_2ZrCl_2 molecules reacted with the internal silanols to incorporate the framework Zr species, in consistent with the FT-IR spectra.

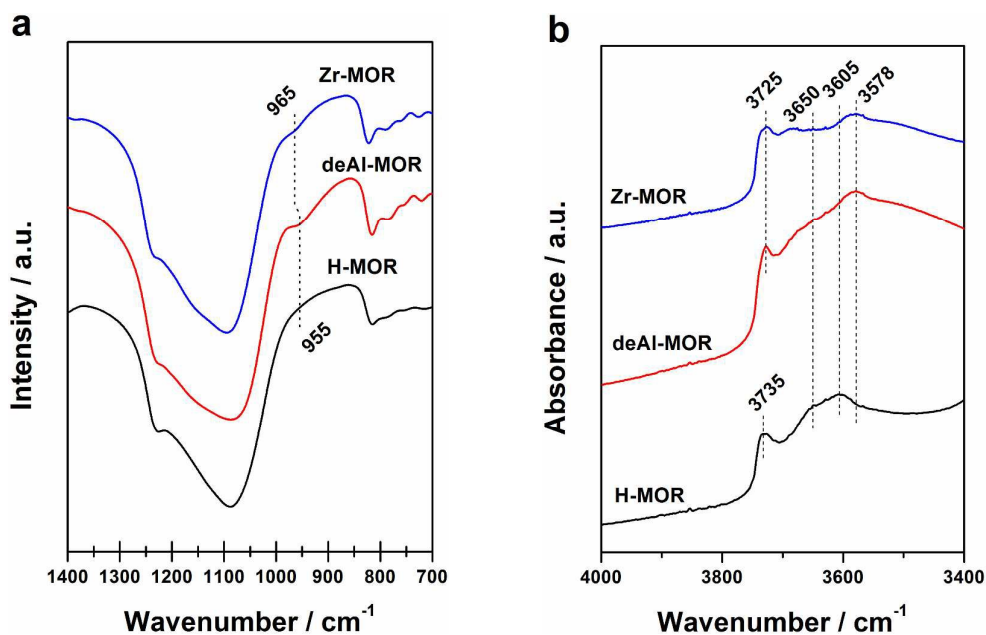


Fig. 5 FTIR (a) and DRIFT (b) spectra of H-MOR, deAl-MOR and Zr-MOR.

3.4 Catalytic activity of Zr-MOR in the ring-opening of epoxides with amines

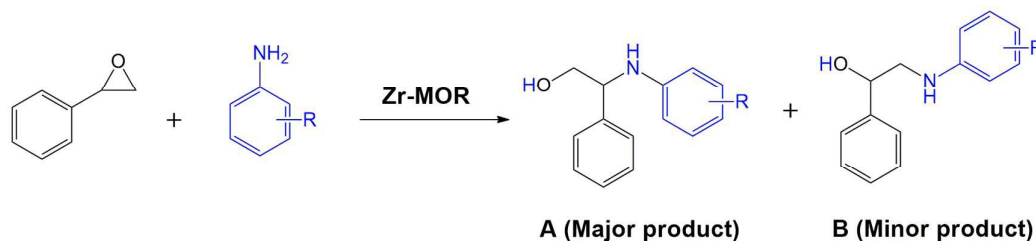
In order to assess the catalytic performance of post-synthesized Zr-MOR, the ring-opening of styrene oxide with aniline was initially investigated under solvent-free conditions (**Table 2**). In the present study, two regio-isomer β -amino alcohols, i.e. 2-phenyl-2-(phenylamino)ethanol and 1-phenyl-2-(phenylamino)-ethanol, were observed as the major and minor products, respectively, as illustrated in **scheme 2**. Blank experiment showed very low styrene oxide conversion (< 7%) with nearly the same selectivity to regio-isomer A (56.3%) and B (43.7%). Negligible increase in the product was gained when using H-MOR or deAl-MOR as catalyst. Dealuminated zeolite supported oxides like $\text{ZrO}_2/\text{deAl-MOR}$, $\text{SnO}_2/\text{deAl-MOR}$ and $\text{TiO}_2/\text{deAl-MOR}$ worked in the epoxide ring-opening process but gave poor reactivity. Interestingly, the incorporation of metal ions (Sn^{4+} , Ti^{4+} or Zr^{4+}) into the MOR framework resulted into considerable styrene oxide conversion as well as high regio-isomer A selectivity. This could be due to the fact that these ions in zeolite framework could serve as Lewis acid sites to adsorb and activate the epoxide substrates [27,28]. Compared with Sn-MOR and Ti-MOR analogues, Zr-MOR showed a much higher catalytic performance, achieving 90.2% styrene oxide conversion and 93.1% regio-isomer A selectivity. This result indicated the unique

activity of framework-incorporated Zr sites for the ring-opening aminolysis of epoxides reaction. In our previous work, it was found that the ring-opening aminolysis of reaction reactivity depended largely on the nature of active sites of catalysts [38]. Both the strong Lewis acidity of Sn⁴⁺ sites and Ti⁴⁺ sites with weak Lewis acidity led to a stronger adsorption of aniline over styrene oxide, which was fatal for the activation of epoxide, a key step in the ring-opening process. As a result, Zr⁴⁺ sites with moderate Lewis acidity represented the advantage on the catalytic ring-opening of epoxide. This maybe a plausible explanation for the reactivity order of Zr-MOR > Ti-MOR > Sn-MOR in this study. Moreover, the TON value of Zr-MOR was estimated to be 1050, even higher than our previously reported hierarchical Zr-Beta zeolite (TON = 939).

Table 2 Aminolysis of styrene oxide with aniline over various zeolite catalyst^a

Catalyst	Styrene oxide conv. ^b (%)	β-Amino alcohols select. ^b (%)		TON ^c (mol _{Epo} mol _M ⁻¹)
		A	B	
		None	< 7	
H-MOR	9.0	51.8	48.2	—
deAl-MOR	8.3	52.3	47.7	—
SnO ₂ /deAl-MOR	9.8	83.8	16.2	117
TiO ₂ /deAl-MOR	12.5	84.1	15.9	147
ZrO ₂ /deAl-MOR	15.6	88.0	12.0	182
Sn-MOR	48.5	90.5	9.5	563
Ti-MOR	65.8	91.9	8.1	767
Zr-MOR	90.2	93.1	6.9	1050

^a Reaction conditions: 5 mmol styrene oxide; 5 mmol aniline, 25 mg catalyst, temperature = 313 K, reaction time = 4 h. ^b Experimental accuracy of ± 2% from GC analysis. ^c TON = moles of styrene oxide converted per mole of the metal center.



Scheme 2 Ring-opening of styrene oxide with amines for synthesis of β -amino alcohols.

The influence of reaction parameters (*e.g.* role of solvent, $n_{\text{Si}}/n_{\text{Zr}}$ ratio, reaction temperature and reaction time) were investigated in this study. As given in **Table 3**, catalytic activity of Zr-MOR zeolite was found to be rather higher when reaction was conducted in the absence of solvent. Decrease in the catalytic activity was observed once solvent was used, and more evident in polar aprotic solvent than non-polar solvent. This difference in reactivity could be related to the adsorption of solvent molecules on the catalytic active sites (*i.e.* Lewis acid sites). In the absence of solvent, only reactant molecules were accessible to the active sites and activated, while solvent molecules, especially polar solvent solvents could mask the active sites ascribed to the competitive adsorption of reactant and solvent molecules, which hindered the interaction between the catalytic sites and the reactant molecules, thus leading to the lowered catalytic activity.

Table 3 Influence of solvent on the aminolysis of styrene oxide with aniline^a

Solvent	Styrene oxide conv. ^b (%)	β -Amino alcohols select. ^b (%)		TON ^c (mol _{Epo} mol _M ⁻¹)
		A	B	
None	90.2	93.1	6.9	1050
Toluene	81.5	93.4	6.6	949
CH ₂ Cl ₂	68.3	93.0	7.0	795
CHCl ₃	69.6	93.1	6.9	810
CCl ₄	83.7	93.8	6.2	974
CH ₃ CN	40.5	92.8	7.2	471

^a Reaction conditions: 5 mmol styrene oxide; 5 mmol aniline, 5 mL solvent; 25 mg catalyst, temperature = 313 K, reaction time = 4 h. ^b Experimental accuracy of $\pm 2\%$

from GC analysis. ^c TON = moles of styrene oxide converted per mole of the metal center.

The $n_{\text{Si}}/n_{\text{Zr}}$ ratio exhibited great impact on the catalytic performance of Zr-MOR in the ring-opening aminolysis of styrene oxide reaction (**Table 4**). A big improvement in conversion of styrene oxide from 40.5 to 90.2% was gained when increasing the $n_{\text{Si}}/n_{\text{Zr}}$ ratio in Zr-MOR from 200 to 100. However, further increasing the Zr loading only resulted in a marginal increase in the styrene oxide conversion (91.6% for Zr-MOR-50 and 92.0% for Zr-MOR-25, respectively). To reveal the intrinsic activity of as-prepared Zr-MOR zeolites, the productivity based on Zr were taken into consideration. Similar productivity was obtained for Zr-MOR-100 (447.2 $\text{gAg}^{-1}\text{Zr h}^{-1}$) and Zr-MOR-200 (402.4 $\text{gAg}^{-1}\text{Zr h}^{-1}$), which was distinctly higher than those of Zr-MOR-50 (226.3 $\text{gAg}^{-1}\text{Zr h}^{-1}$) and Zr-MOR-25 (113.9 $\text{gAg}^{-1}\text{Zr h}^{-1}$). This result indicated the fact that it was approaching saturation of framework Zr in MOR zeolite at $n_{\text{Si}}/n_{\text{Zr}}$ ratio of 100, and more Zr species would be forced to locate non-framework positions and form oxides, lowering the catalytic activity.

Table 4 Influence of $n_{\text{Si}}/n_{\text{Zr}}$ ratio on the aminolysis of styrene oxide with aniline^a

$n_{\text{Si}}/n_{\text{Zr}}$ ratio	Styrene oxide conv. ^b (%)	β -Amino alcohols select. ^b (%)		Productivity ($\text{gAg}^{-1}\text{Zr h}^{-1}$)	TON ^c (mol_{Epo} $\text{mol}_{\text{M}}^{-1}$)
		A	B		
200	40.5	93.3	6.7	402.4	943
100	90.2	93.1	6.9	447.2	1050
50	91.6	92.8	7.2	226.3	533
25	92.0	93.0	7.0	113.9	268

^a Reaction conditions: 5 mmol styrene oxide; 5 mmol aniline, 5 mL solvent; 25 mg catalyst, temperature = 313 K, reaction time = 4 h. ^b Experimental accuracy of $\pm 2\%$ from GC analysis. ^c TON = moles of styrene oxide converted per mole of the metal center.

Fig. 6 showed the influence of reaction temperature and reaction time on the ring-opening aminolysis reaction. As the temperature increased from 303 to 333 K,

the styrene oxide conversion increased from 54.9 to 100%. The reaction proceeded much faster with higher temperature, however, adversely affecting the product proportion. There was a margin decrease in the product A selectivity, indicating at higher temperature product A could isomer into B on the acidic sites (**Fig. 6a**). It was worth noting that, different from most traditional process, the ring-opening aminolysis of styrene oxide occurred even under ambient temperature (303 K) with high yield and selectivity for product A, suggesting the high catalytic efficiency of as-synthesized Zr-MOR zeolite. As represented in **Fig. 6b**, the styrene oxide conversion increased steadily with prolonging the duration time in 4 h, and the maximum conversion was observed at ca. 91.0% with the product A selectivity of 93.1%. Further increase in the reaction time could not exert obvious influence on the ring-opening aminolysis process.

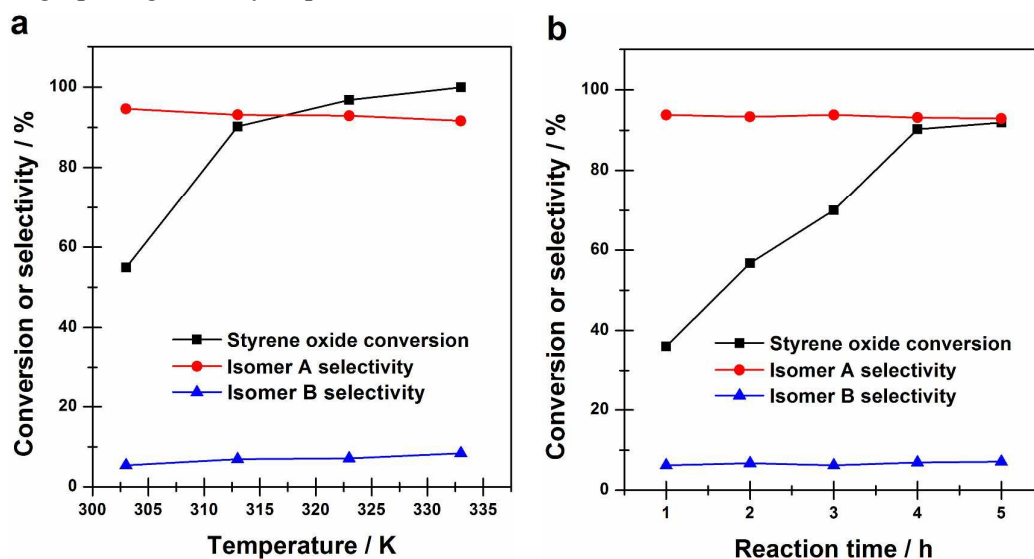
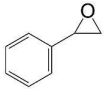
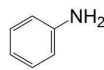
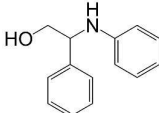
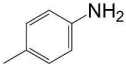
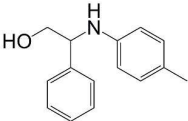


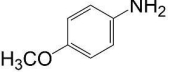
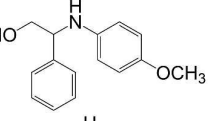
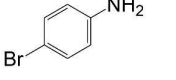
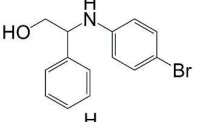
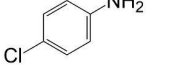
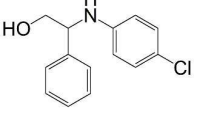
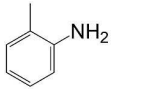
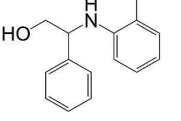
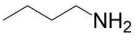
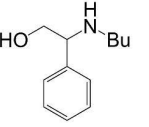
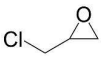
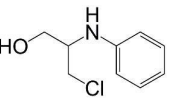
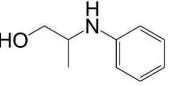
Fig. 6 Influence of reaction temperature (a) and reaction time (b) on the ring-opening aminolysis of epoxides reaction. Reaction conditions: styrene oxide, 5 mmol; aniline, 5 mmol; catalyst amount, 25 mg; reaction time, 4h for a; reaction temperature, 313 K for b.

After optimisation of the reaction parameters, the ring-opening aminolysis reaction was further investigated to broad the substrate scope by using different epoxide and amine reactants with Zr-MOR as the catalyst, and the results were summarized in **Table 5**. Amongst the amine substrates investigated, aniline was found to be the most

active one, achieving 90.2% styrene oxide conversion with 93.1% β -amino alcohol selectivity, which showed much higher activity than the substituted amines. In contrast to aniline, very low styrene oxide conversion and unsatisfactory regio-selectivity were afforded with aliphatic primary amine, such as *n*-butylamine. Similar phenomenon has also been reported in the titanosilicates catalytic system [26,27]. To explain such a result, a good correlation between the aminolysis rate and the basicity, i.e. pK_a value, of the amine was plotted in **Fig. 7**. As can be seen, the epoxide ring-opening rate decreased with increasing pK_a value of amine. It was accepted that ring-opening aminolysis of epoxide was a bimolecular reaction, in which there should be an optimal bonding between the active sites of catalyst and the two reactant molecules [27]. However, when amine with higher pK_a value was used as the substrate, it would be strongly bonded to the Zr^{4+} sites, thus lowering their ability to further activate epoxide molecules. Taking *n*-butyl amine ($pK_a = 10.6$) as an example, it just showed a very low conversion (7.1%), much lower than 4-chloroaniline ($pK_a = 4.0$) with the conversion high up to 72.5%. On the other hand, the reactivity was determined to be in the sequence of styrene oxide > epichlorohydrin > propene oxide. Trends in the catalytic activity could be ascribed to the higher epoxide/amine adsorption ratio for styrene oxide than the other two epoxides [28]. From the results discussed above, it could be inferred that preferential adsorption and activation of epoxide were the key step in ring-opening aminolysis of epoxide reaction.

Table 5 Aminolysis of epoxides with amines Zr-MOR zeolite^a

Epoxide	Amine	β -amino alcohol	Epoxide conv. ^b (%)	Select. ^b (%)	TON ^c (mol _{Epo} mol _M ⁻¹)
			90.2	93.1	1050
			58.3	91.2	679

		49.4	91.5	575
		74.1	94.8	863
		72.5	93.1	844
		65.8	91.0	766
		7.1	26.8	83
		63.4	92.6	738
		51.6	80.8	601

^a Reaction conditions: 5 mmol epoxide; 5 mmol amine; 25 mg catalyst, temperature = 313 K, reaction time = 4 h. ^b Experimental accuracy of $\pm 2\%$ from GC analysis. ^c TON = moles of styrene oxide converted per mole of the metal center.

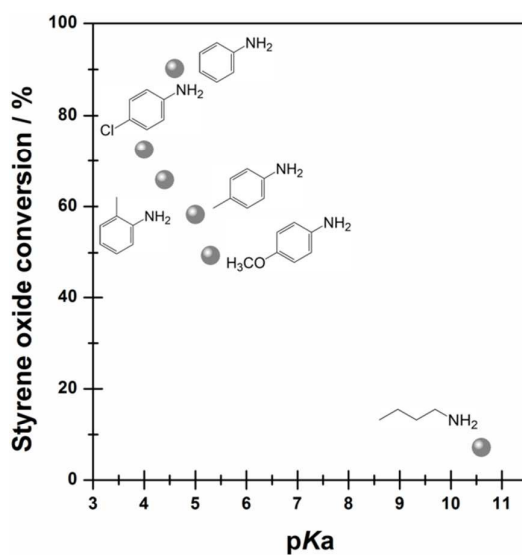


Fig. 7 Correlation between the catalytic activity and the pKa value of amines in the

ring-opening aminolysis of styrene oxide reaction. Reaction conditions: styrene oxide, 5 mmol; aniline, 5 mmol; catalyst amount, 25 mg; reaction temperature, 313 K; reaction time, 4h.

To confirm the true heterogeneity of as-synthesized Zr-MOR, a hot-filtration experiment was conducted to determine if active components could leach into the reaction mixture and possibly participated in the catalytic ring-opening aminolysis reaction. As shown in **Fig. 8**, the β -amino alcohol yield reached ca. 34% after 1 h, then the catalyst was immediately removed from the reaction system, and the mother liquor was allowed to proceed for another 3 h under the identical reaction conditions. Obviously, removal of the catalyst led to the complete termination of the reaction, verifying the truly heterogeneous nature of the ring-opening aminolysis process over Zr-MOR.

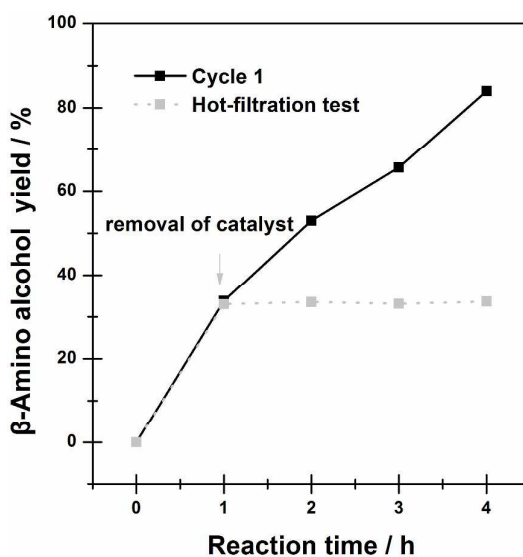


Fig. 8 β -Amino alcohol yield in the ring-opening of styrene oxide with aniline over Zr-MOR. Reaction conditions: styrene oxide, 5 mmol; aniline, 5 mmol; reaction temperature, 313 K.

Catalyst stability and the feasibility of recycling was a very important factor for heterogeneous catalysis. To this end, the ring-opening of styrene oxide with aniline reaction was investigated in successive runs over Zr-MOR (the catalyst was pre-calcinated for the next use), and the results were presented in **Fig. 9**. As can be seen, there was no obvious change in the catalytic activity and product selectivity

even after six successive recycling. The possible leaching of Zr species into reaction medium as well as change in the texture properties of Zr-MOR after cycles were excluded by ICP analysis (**Table S1**), XRD and surface area characterization (**Fig. S3** & **Table S1**), respectively. These results emphasized the fact that Zr-MOR prepared by the post-synthesis dry impregnation strategy in this study serves as a potential heterogeneous catalyst for the ring-opening aminolysis of epoxides.

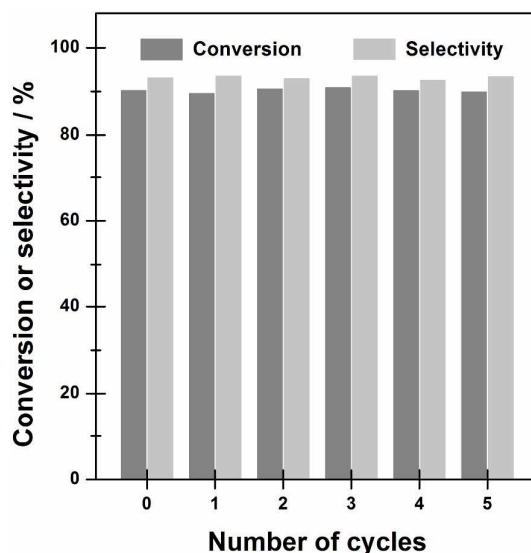


Fig. 9 Recycling test for the ring-opening of styrene oxide with aniline over Zr-MOR.

Reaction conditions: 5 mmol; aniline, 5 mmol; catalyst amount, 25 mg; reaction temperature, 313 K; reaction time, 4h.

4 Conclusions

In the present study, Zr-MOR zeolite has been prepared using a two-step post-synthesis strategy, in which the incorporation of Zr atom into the framework of MOR zeolite involved creating defect sites associated with silanol groups via dealumination and subsequent interaction of these silanol groups with the corresponding Cp_2ZrCl_2 precursor. Characterization results from UV-vis and XPS analysis confirmed that the incorporated Zr species were in tetrahedrally coordinated configuration. For the ring-opening aminolysis of epoxides reaction, as-prepared Zr-MOR exhibited much higher catalytic activity in comparison with Sn- and Ti-silicate analogues. The catalytic aminolysis activity depended much on the pKa value of amines and the adsorption abilities of reactant molecules. The hot-filtration

and recycling experiments revealed the true heterogeneity and perfect stability of Zr-MOR prepared by post-synthesis procedures.

Acknowledgment

This work was financially supported by the NSFC (Grants 21531005, 21401140) and the 973 program (2014CB845601). The support from the doctoral program foundation of Tianjin Normal University (52XB1509) and the program for Innovative Research Team in University of Tianjin (TD12-5038) were also acknowledged.

References

- [1] T. Punniyamurthy, S. Velusamy and J. Iqbal, *Chem. Rev.*, 2005, **105**, 2329.
- [2] J. H. Huang, T. Akita, J. Faye, T. Fujitani, T. Takei and M. Haruta, *Angew. Chem. Int. Ed.*, 2009, **48**, 7862.
- [3] O. Mitsunobu, in: B. M. Trost, I. Fleming, (Eds.), *Comprehensive organic synthesis*, vol. 6, Springer, New York, 1991, p. 88.
- [4] D. J. Ager, I. Prakash and D. R. Schaad, *Chem. Rev.*, 1996, **96**, 835.
- [5] E. J. Corey and F. Y. Zhang, *Angew. Chem. Int. Ed.*, 1999, **38**, 1931.
- [6] P. O'Brien, *Angew. Chem. Int. Ed.*, 1999, **38**, 326.
- [7] A. Procopio, M. Gaspari, M. Nardi, M. Oliverio and O. Rosati, *Tetrahedron Lett.*, 2008, **49**, 2289.
- [8] S. V. Malhotra, R. P. Andal and V. Kumar, *Synth. Commun.*, 2008, **38**, 4160.
- [9] M. J. Bhanushali, N. S. Nandurkar, M. D. Bhor and B. M. Bhanage, *Tetrahedron Lett.*, 2008, **49**, 3672.
- [10] M. Moghadam, S. Tangestaninejad, V. Mirkhani, I. Mohammadpoor-Baltork, S. Gorjipoor and P. Yazdani, *Synth. Commun.*, 2009, **39**, 552.
- [11] A. K. Chakraborti and A. Kondaskar, *Tetrahedron Letter.*, 2003, **44**, 8315.
- [12] M. Curini, F. Epifano, M. C. Marcotullio and O. Rosati, *Eur. J. Org. Chem.*, 2001, 4149.
- [13] W. M. Xue, M. C. Kung, A. I. Kozlov, K. E. Popp and H. H. Kung, *Catal. Today*, 2003, **85**, 219.

- [14] A. K. Chakraborti, A. Kondaskar and S. Rudrawar, *Tetrahedron*, 2004, **60**, 9085.
- [15] R. I. Kureshy, S. Singh, N. H. Khan, S. H. R. Abdi, E. Suresh and R. V. Jasra, *J. Mol. Catal. A*, 2007, **264**, 162.
- [16] M. M. Heravi, B. Baghernejad and H. A. Oskooie, *Catal. Lett.*, 2009, **130**, 547.
- [17] J. Liang, Z. B. Liang, R. Q. Zou and Y. L. Zhao, *Adv. Mater.*, 2017, **29**, 1701139.
- [18] A. Corma, L. T. Nemeth, M. Renz and S. Valencia, *Nature*, 2001, **412**, 423.
- [19] D. Mehlhorn, A. Inayat, W. Schwieger, R. valiullin and J. Karger, *ChemPhysChem*, 2014, **15**, 1681.
- [20] D. Makee, US 3140931 (1964).
- [21] Q. H. Xia, H. Q. Ge, C. P. Ye, Z. M. Liu and K. X. Su, *Chem. Rev.*, 2005, **105**, 1603.
- [22] A. Corma, H. Garcia, *Chem. Rev.*, 2003, **103**, 4307.
- [23] Y. Roman-Leshkov and M. E. Davis, *ACS Catal.*, 2011, **1**, 1566.
- [24] D. Zhou, T. J. Zhang, Q. H. Xia, Y. R. Zhao, K. X. Lv, X. H. Lu and R. F. Nie, *Chem. Sic.*, 2016, **7**, 4966.
- [25] J. K. Satyarthi, L. Saikia, D. Srinivas and P. Ratnasamy, *Appl. Catal. A*, 2007, **330**, 145.
- [26] L. Saikia, J. K. Satyarthi, D. Srinivas and P. Ratnasamy, *J. Catal.*, 2007, **252**, 148.
- [27] A. Kumar and D. Srinivas, *J. Catal.*, 2012, **293**, 126.
- [28] R. Kore, R. Srivastava and B. Satpati, *ACS Catal.*, 2013, **3**, 2891.
- [29] I. E. Maxwell and W. H. J. Stork, in: H. V. Bekkum, E. M. Flanigen, J. C. Jonsen (Eds.), *Introduction to zeolite Science and Practise*, Elsevier, Amsterdam, 1991, p. 71.
- [30] P. Li, G. Q. Liu, H. H. Wu, Y. M. Liu, J. G. Jiang and P. Wu, *J. Phys. Chem. C*, 2011, **115**, 3663.
- [31] C. Hammond, S. Conrad and I. Hermans, *Angew. Chem. Int. Ed.*, 2012, **51**, 11736.
- [32] X. M. Yang, L. Wu, Z. Wang, J. J. Bian, T. L. Lu, L. P. Zhou, C. Chen and J. Xu, *Catal. Sci. Technol.*, 2016, **6**, 1757.
- [33] J. Zhang, L. Wang, G. X. Wang, F. Chen, J. Zhu, C. T. Wang, C. Q. Bian, S. X.

- Pan and F. S. Xiao, *ACS Sustainable Chem. Eng.*, 2017, **5**, 3123.
- [34] Q. Guo, F. Fan, E. A. Pidko, W. N. Graaff, Z. Feng, C. Li and E. J. Hensen, *ChemSusChem*, 2013, **6**, 1352.
- [35] W. L. Dai, C. M. Wang, B. Tang, G. J. Wu, N. J. Guan, Z. K. Xie, M. Hunger and L. D. Li, *ACS Catal.*, 2016, **6**, 2955.
- [36] B. Tang, W. L. Dai, G. J. Wu, N. J. Guan, L. D. Li and M. Hunger, *ACS Catal.*, 2014, **4**, 2801.
- [37] B. Tang, W. L. Dai, X. M. Sun, N. J. Guan, L. D. Li and M. Hunger, *Green Chem.*, 2014, **16**, 2281.
- [38] B. Tang, W. L. Dai, X. M. Sun, G. J. Wu, N. J. Guan, M. Hunger and L. D. Li, *Green Chem.*, 2015, **17**, 1744.
- [39] P. Wu, T. Komatsu and T. Yashima, *J. Phys. Chem.*, 1995, **99**, 10923.
- [40] H. Xu, Y. T. Zhang, H. H. Wu, Y. M. Liu, X. H. Li, J. G. Jiang, M. Y. He and P. Wu, *J. Catal.*, 2011, **281**, 263.
- [41] M. S. Morey, G. D. Stucky, S. Schwarz and M. Fröba, *J. Phys. Chem. B*, 1999, **103**, 2037.
- [42] J. E. Haskouri, S. Cabrera, C. Guillem, J. Latorre, A. Beltrán, B. Beltrán, M. D. Marcos and P. Amorós, *Chem. Mater.*, 2002, **14**, 5015.
- [43] A. Ramanathan, M. C. C. Villalobos, C. Kwakernaak, S. Telalovic and U. Hanefeld, *Chem. Eur. J.*, 2008, **14**, 961.
- [44] V. L. Sushkevich, I. I. Ivanova, S. Tolborg and E. Taarning, *J. Catal.*, 2014, **316**, 121.
- [45] J. J. Pacheco and M. E. Davis, *Proc. Natl. Acad. Sci.*, 2014, **111**, 8363.
- [46] B. Rakshe, V. Ramaswamy, S. G. Hegde, R. Vetrivel and A. V. Ramaswamy, *Catal. Lett.*, 1997, **45**, 41.
- [47] G. G. Juttu and R. F. Lobo, *Catal. Lett.*, 1999, **62**, 99.
- [48] B. Rakshe, V. Ramaswamy, S. G. Hegde, R. Vetrivel and A. V. Ramaswamy, *Catal. Lett.*, 1997, **45**, 41.
- [49] R. Szostak, in: *Molecular sieves: principles of synthesis and identification*, Van Nostrand Reinhold, New York, 1989, p. 317.

- [50] P. Wu, T. Komatsu and T. Yashima, *J. Phys. Chem.*, 1998, **102**, 9297.
- [51] G. L. Woolery, L. B. Alemany, R. M. Dessau and A. W. Chester, *Zeolites*, 1986, **6**, 14.
- [52] Z. G. Zhu, H. Xu, J. G. Jiang, X. Liu, J. H. Ding and P. Wu, *Appl. Catal. A*, 2016, **519**, 155.

Figures caption

Fig. 1 Wide angle XRD patterns (a) and enlarged (200) reflections (b) of H-MOR, deAl-MOR and Zr-MOR.

Fig. 2 SEM images and EDS mapping of Si and Zr for Zr-MOR.

Fig. 3 UV-vis spectra of Zr-MOR and ZrO₂.

Fig. 4 Zr 3d XPS of Zr-MOR and ZrO₂.

Fig. 5 FTIR (a) and DRIFT (b) spectra of H-MOR, deAl-MOR and Zr-MOR.

Fig. 6 Influence of reaction temperature (a) and reaction time (b) on the ring-opening aminolysis of epoxides reaction. Reaction conditions: styrene oxide, 5 mmol; aniline, 5 mmol; catalyst amount, 25 mg; reaction time, 4h for a; reaction temperature, 313 K for b.

Fig. 7 Correlation between the catalytic activity and the pK_a value of amines in the ring-opening aminolysis of styrene oxide reaction. Reaction conditions: styrene oxide, 5 mmol; aniline, 5 mmol; catalyst amount, 25 mg; reaction temperature, 313 K; reaction time, 4h.

Fig. 8 β-Amino alcohol yield in the ring-opening of styrene oxide with aniline over Zr-MOR. Reaction conditions: styrene oxide, 5 mmol; aniline, 5 mmol; reaction temperature, 313 K.

Fig. 9 Recycling test for the ring-opening of styrene oxide with aniline over Zr-MOR. Reaction conditions: 5 mmol; aniline, 5 mmol; catalyst amount, 25 mg; reaction temperature, 313 K; reaction time, 4h.

Post-synthesis of Zr-MOR as robust solid acid catalyst for the ring-opening aminolysis of epoxides

